High-Energy Mode-Locked All-Fiber Laser with Ultralong Resonator

S. M. Kobtsev*, S. V. Kukarin, S. V. Smirnov, and Y. S. Fedotov

Novosibirsk State University, ul. Pirogova 2, Novosibirsk, 630090 Russia

*e-mail: kobtsev@lab.nsu.ru

Received June 15, 2009

Abstract—The first experimental results on an all-fiber mode-locked ytterbium laser whose ultralong cavity has a length of 8 km are presented. An increase in the length of the laser cavity at a constant mean power of radiation makes it possible to increase the pulse energy by more than two orders of magnitude to a level of 4 μJ, which is record-high for the pulses generated by a fiber mode-locked master oscillator in the absence of Q-switching. A pulse repetition rate of 37 kHz is the record-low repetition rate for the mode-locked lasers. The numerical simulation of the lasing in the absence of extension fiber yields a possibility of a wide-range variation in the pulse duration due to the tuning of the intracavity polarization controllers. The simulation results are in qualitative agreement with the experimental data.

INTRODUCTION

Various methods are used to generate laser pulses with relatively high energies. Several methods make it possible to increase the radiation pulse energy in the laser, and alternative approaches enable one to increase the pulse energy using external optical amplifiers. The Q-switching [1–3] and the cavity dumping of the mode-locked laser [4] are the most widely spread methods for the generation of high-energy pulses in lasers. An increase in the pumping power of the master oscillator also leads to an increase in the pulse energy but such an approach has several limitations [5]. In the conventional mode-locked lasers, the main attention is paid to the generation of relatively short pulses, and pulse energies ranging from 10 to 25 nJ were recently considered as relatively high pulse energies [6–8]. The record-high pulse energies attained in the mode-locked fiber lasers in the absence of amplification were higher by an order of magnitude: 120–265 nJ [9–11].

Another method for an increase in the pulse energy involves a decrease in the pulse repetition rate of the mode-locked laser owing to an increase in the cavity length at the same mean power of radiation. Such an approach can be easily implemented in fiber lasers, whose cavity length can be easily increased without negative effects on the stability of lasing. Note that this method is also employed in solid-state mode-locked lasers [12–14]. For the first time, the cavity of the mode-locked fiber laser was extended for an increase in the pulse energy in [9]. An increase in the cavity length by 400 m led to an increase in the pulse energy to 120 nJ. Solid-state and fiber lasers with the mode-locking in the cavities with lengths of 100 m were demonstrated in [12, 15].

In previous work [16], we demonstrated a possibility of the stable mode-locking in a discrete fiber laser with an optical length of the cavity of 3.8 km. Such a mode-locked laser exhibits both an ultralong cavity and a record-high energy of 3.9 μJ for the pulses generated in the laser at an ultralow repetition rate of 77 kHz.

In this work, we develop the method for an increase in the pulse energy and present the first results on the mode-locking in an all-fiber Yb laser with an optical cavity length of 8 km providing a record-high pulse energy of 4 μJ at a pulse duration of 10 ns and a minimum (for the mode-locked lasers) pulse repetition rate of 37 kHz. For the first time, the parameters of such a mode-locked laser appear close to the parameters of a Q-switched laser with respect to the pulse energy, duration, and repetition rate.

EXPERIMENT

Figure 1 demonstrates the scheme of the ultralong all-fiber laser. We employ the ring cavity in which the radiation is outcoupled from the cavity via a fiber polarization splitter. The non-polarization-maintaining cladding-pumped Yb-doped fiber serves as the active medium of the laser that is pumped via a multimode coreless fiber [17]. The length of the active Yb-doped fiber is 10 m, and the core diameter is 7 μm. The active fiber is pumped by a multimode diode laser with an output power of up to 1.5 W at a wavelength of 980 nm.

The mode-locking of such a laser is performed using the nonlinear polarization rotation [18–20]. Two fiber polarization controllers provide the needed polarization. An SMF-28 fiber is used for an increase in the cavity length. The maximum output power of
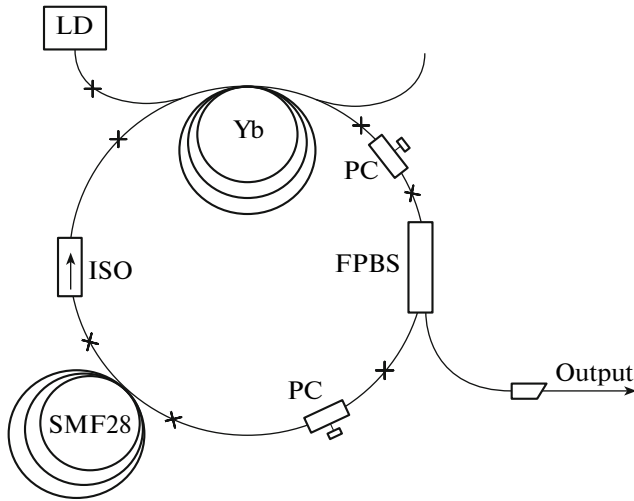
Fig. 1. Scheme of the all-fiber mode-locked ring Yb laser with the ultralong (8 km) cavity: LD pumping laser diode, PC fiber polarization controller, ISO polarization-insensitive optical isolator, and FPBS fiber polarization beam splitter.

the laser (150 mW) is limited by the allowed power of the output polarization beam splitter.

Figure 2 shows the autocorrelation functions (ACFs) of the pulses for the laser with the short (unextended) cavity. The double (femtosecond–picosecond) structure (Fig. 2a) is typical of the pulses generated in the short cavity. The width of the picosecond base of the ACF is 6 ps, and the duration of the femtosecond component of the ACF is no greater than 170 fs. Figure 2b demonstrates the interference ACF of the femtosecond component. The compression of such pulses using two diffraction gratings allows a decrease in the duration of the picosecond component but the duration of the femtosecond component

increases. Figure 3 shows the ACF of the compressed pulses with a width of no greater than 800 fs. On the assumption of the Gaussian pulse shape, the pulse duration is about 560 fs. The measured spectral width of the radiation of the short-cavity laser with a central wavelength of 1087 nm is 3 nm, which proves the bandwidth-limited character of the compressed pulses.

For an increase in the cavity length, we employ the conventional SMF-28 fiber with a length of 5.46 km. With such an extension, the optical length of the laser cavity is 8 km. In the long-cavity laser (as well as in the short-cavity laser), the stable mode-locking is reached due to the tuning of the polarization controllers. Figures 4 and 5 demonstrate the time distribution and spectrum of the radiation of the long-cavity laser, respectively. The laser generates a pulse train with a pulse duration of 10 ns and a spectral width of 0.44 nm. The central wavelength of the long-cavity laser (1080.1 nm) is blue-shifted by about 7 nm relative to the central wavelength of the short-cavity laser. The mean output power of the long-cavity laser is also no greater than 150 mW. The pulse repletion rate (37 kHz) is record-low for the mode-locked lasers. At the maximum mean output power (150 mW), the pulse energy (4.05 μJ) is record-high for the fiber master oscillators in the absence of amplification and Q-switching.

Note that a relatively large pulse duration of the long-cavity laser (10 ns) is related to the gigantic phase modulation owing to the positive dispersion of the laser cavity. The pulses can be compressed but the optimal technical implementation of the compensation for such an enormous phase modulation remains unclear.

Generalizing the above data and the results from [16], we arrive at an increase in the laser pulse duration with an increase in the cavity length: the pulse dura-
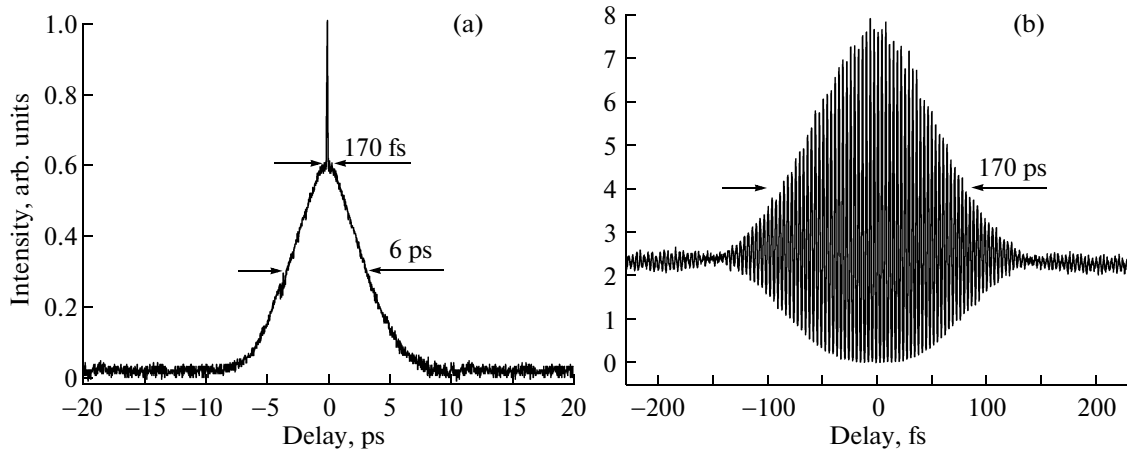

Fig. 2. ACFs of the output pulses of the short-cavity laser: (a) noncollinear ACF and (b) interference ACF of the central part of the pulse.

tion is 3 ns for a cavity length of 3.8 km [16] and the pulse duration is 10 ns for a length of 8 km. Thus, the proposed configuration allows a variation in the laser pulse duration with a variation in the cavity length. In addition, the simulation results (see below) show that the pulse duration can be varied in wide ranges at a constant cavity length due to the tuning of the polarization controllers. This effect is observed in the experiments with the short- and long-cavity lasers.

SIMULATION

For the numerical simulation of the lasing in the all-fiber all-positive-dispersion mode-locked laser that employs the nonlinear polarization rotation, we use a system of two nonlinear Schrödinger equations describing the propagation of polarized radiation in fibers in the absence of the linear birefringence [21]:

$$\frac{\partial A_x}{\partial z} + \frac{i}{2}\beta_2\frac{\partial^2 A_x}{\partial t^2} + \frac{\alpha}{2}A_x$$
$$= i\gamma\left(|A_x|^2 + \frac{2}{3}|A_y|^2\right)A_x + \frac{i\gamma}{3}A_x^*A_y^2, \tag{1}$$

$$\frac{\partial A_y}{\partial z} + \frac{i}{2}\beta_2\frac{\partial^2 A_y}{\partial t^2} + \frac{\alpha}{2}A_y$$
$$= i\gamma\left(|A_y|^2 + \frac{2}{3}|A_x|^2\right)A_y + \frac{i\gamma}{3}A_y^*A_x^2. \tag{2}$$

Here, A_x and A_y are the components of the complex vector envelope of the field strength, t is time, z is the spatial coordinate along the fiber, β_2 is the dispersion coefficient, γ is the nonlinear coefficient, and α is the damping coefficient (or gain at $\alpha < 0$).

We numerically solve Eqs. (1) and (2) using the method of the Fourier splitting with respect to the physical factors [21]. We perform the integration with respect to z along the ring cavity that consists of the passive single-mode fiber (SMF), the active Yb-doped fiber, the polarization controllers (PC1 and PC2), the spectral filter, and the polarization beam splitter (Fig. 6). In the calculations, we use the fiber parameters that are close to the experimental values: lengths of the segments of the SMF and Yb-doped fiber, 6 m; dispersion coefficient, $\beta_2 = 20$ ps²/km; and nonlinear coefficient, $\gamma = 4.7$ (km W)$^{-1}$. For the simulation of the gain saturation, we assume that the gain of the active fiber depends on the energy of the optical radiation in the cavity:

$$g = -\alpha = \frac{g_0}{1 + E/(P_{sat}\tau)}. \tag{3}$$

Here, g is the power-dependent gain of the active fiber, g_0 is the unsaturated gain (about 14 dB), E is the energy of the optical radiation in the cavity, P_{sat} is the satura-
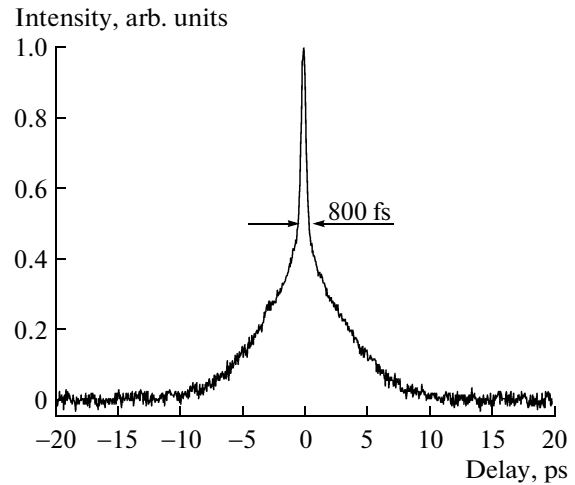

Fig. 3. ACF of the pulses of the short-cavity laser resulting from the pulse compression using two diffraction gratings.
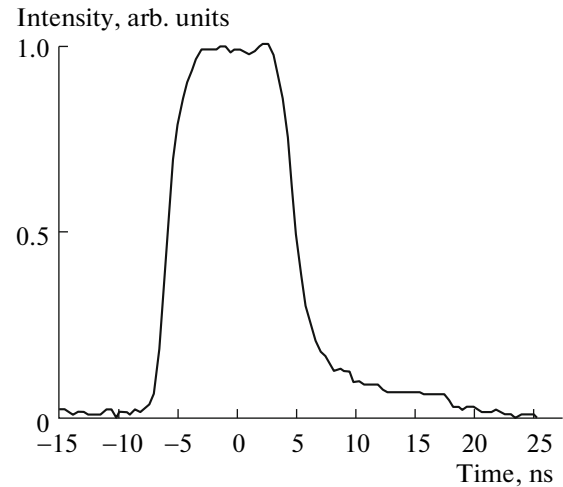

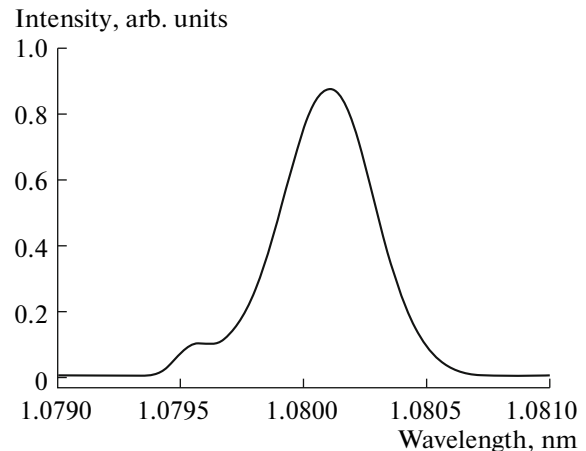**Fig. 4.** Time distribution of the output laser intensity.

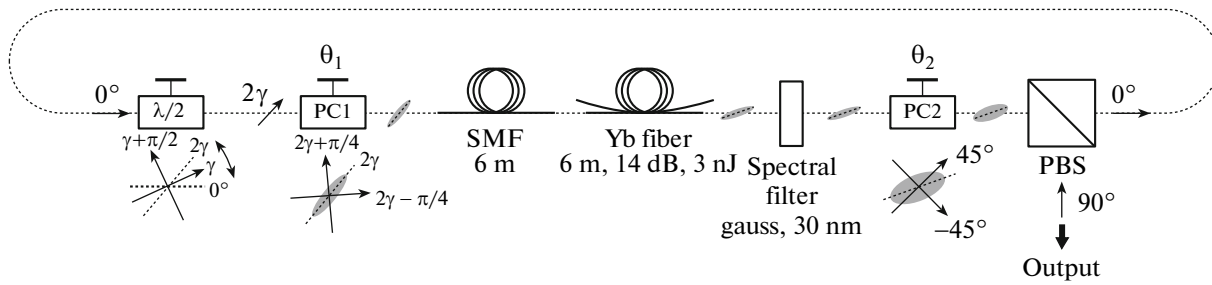**Fig. 5.** Spectrum of the output radiation.

Fig. 6. Numerically simulated evolution of the pulse polarization in the ring cavity.

tion power of the active fiber (about 50 mW), and τ is the round-trip time of the ring cavity. In the calculations, we use a spectral filter with the Gaussian transmission curve centered at about 1064 nm and a width of 30 nm at a transmittance of 1/2. The polarization controllers are described using the unitary unimodular matrices

$$C(\theta, \varphi) = \begin{pmatrix} \cos\dfrac{\theta}{2} - i\sin\dfrac{\theta}{2}\cos 2\varphi & -i\sin\dfrac{\theta}{2}\sin 2\varphi \\ -i\sin\dfrac{\theta}{2}\sin 2\varphi & \cos\dfrac{\theta}{2} + i\sin\dfrac{\theta}{2}\cos 2\varphi \end{pmatrix}, (4)$$

where θ is the difference of the phase shifts introduced by the polarization controller for two linearly polarized states and φ is the orientation of the principal axis of the polarization controller. In the experiments, the polarization controllers have three degrees of freedom.
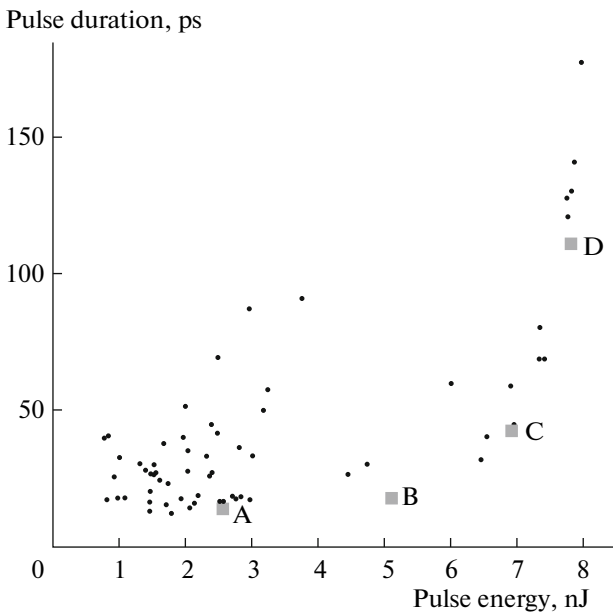

Fig. 7. Spread of the pulse parameters at various tunings of polarization controllers PC1 and PC2 in the scheme in Fig. 6.

Therefore, we calculate polarization controller PC1 in combination with a half-wave retardation plate (Fig. 6), which is described using matrix (4) at θ = π.

To initiate the lasing, we employ the noise field distribution and place one photon with random phase at each mesh point of the reciprocal mesh. At certain tunings of the polarization controllers, we obtain the evolution of the original signal to a single bell-shaped pulse on the mesh over 100–200 round trips of the ring cavity. This result corresponds to the mode-locking and the generation of a periodic pulse train in the experiments. Figure 6 illustrates the evolution of the polarization state of the pulse in the limit cycle of the system of equations (1) and (2). The linear polarization is rotated by half-wave retardation plate and is transformed into the elliptical polarization in polarization controller PC1. The pulse propagation in the passive SMF and the active Yb-doped fiber results in the rotation of the polarization ellipse. The angle of rotation is proportional to the radiation power and the area of the polarization ellipse, which is determined by the tuning of polarization controller PC1. The second polarization controller (PC2) is used to change the ratio of the axes of the polarization ellipse, and, hence, to control the fraction of energy that is outcoupled from the cavity by polarization beam splitter PBS, which transmits the linearly polarized radiation and provides the outcoupling of the orthogonally polarized component. We obtain minimum outcoupling loss for the pulse in the lasing regime and higher loss for the radiation with lower power, so that the system of the intracavity elements works as a saturable absorber and makes it possible to implement the mode-locking.

An interesting feature of the simulation results lies in a relatively large spread of the durations and energies of the generated pulses depending on the tuning of the polarization controllers. In particular, the dots in Fig. 7 show the parameters of the calculated pulses that correspond to various tunings of the polarization controllers. It is seen that the pulse energy and duration exhibit variations by almost an order of magnitude. Figure 8 shows the time dependences of the intensity for four pulses with different parameters.
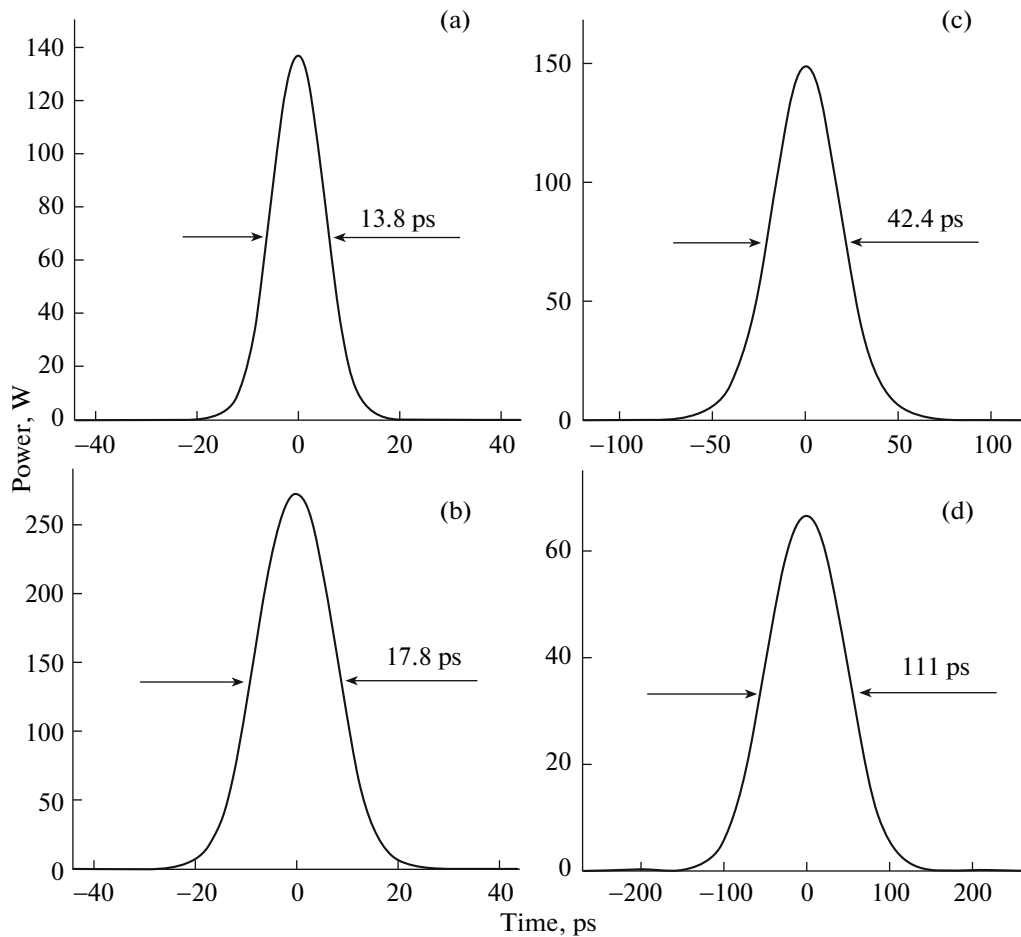
Fig. 8. Plots of the intensity vs. time for four different pulses: panels (a–d) correspond to points in Fig. 7.

Note that the spread of parameters is in qualitative agreement with the above experimental data and the previous experimental results from [16].

radiation for the effective nonlinear spectral conversion or the subsequent amplification in the polarization-maintaining fiber amplifiers.

CONCLUSIONS

An all-fiber mode-locked laser with an ultralong cavity whose length is 8 km is demonstrated for the first time. An increase in the optical length of the optical cavity from 12.5 m to 8 km allows an increase in the pulse energy by more than two orders of magnitude to a level of 4 μJ, which is record-high for the pulses generated by a mode-locked fiber master oscillator in the absence of Q-switching. A variation in the length of such a laser causes a wide-range variation in the pulse duration (from femtoseconds to nanoseconds). The numerical simulation yields a possibility of a significant variation in the pulse duration due to the tuning of the intracavity polarization controllers. Thus, the proposed all-fiber master oscillator offers wide-range variations in the pulse duration, energy, and repetition rate. An additional advantage of the all-fiber laser is the linear polarization of the output radiation. This circumstance makes it possible to employ the laser

REFERENCES

1. J. A. Alvarez-Chavez, H. L. Offerhaus, J. Nilsson, P. W. Turner, W. A. Clarkson, and D. J. Richardson. Opt. Lett. **25**, 37 (2000).

2. S. M. Kobtsev, S. V. Kukarin, and Y. S. Fedotov, Laser Phys. **18**, 1230 (2008).

3. T. Y. Tsai and Y. C. Fang, Opt. Express **17**, 1429 (2009).

4. A. Killi, J. Dörring, U. Morgner, M. Lederer, J. Frei, and D. Kopf, Opt. Express **13**, 1916 (2005).

5. W. Chang, J. M. Soto-Crespo, A. Ankiewicz, and N. Akhmediev, Phys. Rev. A **79**, 033840-1 (2009).

6. A. Hideur, T. Chartier, M. Brunel, S. Louis, C. Ozkul, F. Sanchez, Appl. Phys. Lett. **79**, 3389 (2001).

7. B. Ortac, J. Limpert, and A. Tuennermann, Opt. Lett. **32**, 2149 (2007).

8. F. W. Wise, A. Chong, and W. H. Renninger, Laser Photon. Rev. **2**, 58 (2008).

9. J. U. Kang and R. Posey, Opt. Lett. **23**, 1375 (1998).

10. A. M. Heidt, J. P. Burger, J. N. Maran, and N. Traynor, Opt. Express **15**, 15892 (2007).

11. B. Ortac, O. Schmidt, T. Schreiber, J. Limpert, A. Tuennermann, and A. Hideur, Opt. Express **15**, 10725 (2007).

12. V. Z. Kolev, M. J. Lederer, B. Luther-Davies, and A. V. Rode, Opt. Lett. **28**, 1275 (2003).

13. P. Dombi, P. Antal, J. Fekete, R. Szipocs, and Z. Varallyay, Appl. Phys. B **88**, 379 (2007).

14. P. Dombi and P. Antal, Laser Phys. Lett. **4**, 538 (2007).

15. K. H. Fong, S. Y. Set, and K. Kikuchi, *OFC-2007, March 25−29, Anaheim, CA, OTuF2* (2007).

16. S. Kobtsev, S. Kukarin, and Y. Fedotov, Opt. Express **16**, 21936 (2008).

17. A. B. Grudinin, D. N. Payne, P. W. Turner, L. J. A. Nilsson, M. N. Zervas, M. Ibsen, and M. K. Durkin, Patent USA No. 6 826 335 (November 30, 2004).

18. M. Hofer, M. E. Fermann, F. Haberl, M. H. Ober, and A. J. Schmidt, Opt. Lett. **16**, 502 (1991).

19. V. J. Matsas, T. P. Newson, D. J. Richardson, and D. N. Payne, Electron. Lett. **28**, 1391 (1992).

20. M. E. Fermann, Opt. Lett. **18**, 894 (1993).

21. G. P. Agrawal, *Nonlinear Fiber Optics,* 3rd ed. (Academic, San Diego, SA, 2001).